Estimation of Helix−Helix Association Free Energy from Partial Unfolding of Bacterioopsin†

Suraj John Nannepaga,‡ Ravikumar Gawalapu,‡ Daniel Velasquez,‡ and Robert Renthal*,‡,§

Department of Biology, University of Texas at San Antonio, San Antonio, Texas 78249, and Department of Biochemistry, University of Texas Health Science Center at San Antonio, San Antonio, Texas 78229

Received May 23, 2003; Revised Manuscript Received October 9, 2003

ABSTRACT: To obtain thermodynamic information about interactions between transmembrane helices in integral membrane proteins, partial unfolding of bacterioopsin in ethanol/water mixtures was studied by Förster-type resonance energy transfer (FRET) from tryptophan to a dansyl group on Lys 41. Tryptophan to dansyl FRET was detected by measuring sensitized emission at 490−500 nm from 285 nm excitation. FRET was observed in dansylbacterioopsin in apomembranes and in detergent micelles but not in 90% ethanol/water or in the chymotrypsin fragment C2 (residues 1−71). The main fluorescence donors are Trp 86 and Trp 182. Increase of FRET from C2 with added chymotrypsin fragment C1 (residues 72−248) provides an estimate of the C1−C2 association constant as 7.7×10^6 M^{-1}. With increasing ethanol concentration, the FRET signal from dansylbacterioopsin in detergent micelles disappeared with a sharp transition above 60% ethanol. No transition occurred in Trp fluorescence from bacterioopsin lacking the dansyl acceptor, nor did dansyl model compounds undergo a similar transition. Light scattering measurements show that the detergent micelles dissipate below 50% ethanol. Thus the observed transition is likely to be a partial unfolding of bacterioopsin. Assuming a two-state unfolding model, the free energy of unfolding was obtained by extrapolation as 9.0 kcal/mol. The slope of the transition (*m*-value) was −0.8 kcal mol^{-1} M^{-1}. The unfolding process probably involves dissociation of several helices. The rate of association was measured by stopped-flow fluorometry. Two first-order kinetic processes were observed, having approximately equal weights, with rate constants of 2.32 s^{-1} and 0.185 s^{-1}.

Helix−helix association in a lipid bilayer is an essential step in the folding of many integral membrane proteins (*1*). The protein side chains that are buried at the helix−helix interfaces are about as hydrophobic as those found in the interior of water-soluble proteins (*2*). Furthermore, connecting loops in the aqueous phase are not necessary for transmembrane helix association (*3*−*9*). In some cases, helix association can be driven by polar interactions within the bilayer (*10*−*12*). However, nonpolar helices are also known to associate spontaneously in micelles and lipid bilayers (*13*−*16*). This raises the question as to why transmembrane proteins should form compact structures in the presence of lipids, rather than spreading out to maximize the lipid−helix interactions. It is not clear what thermodynamic processes drive helix−helix association.

A great deal is known about folding of water-soluble proteins. In some small, single-domain proteins, a transition occurs between unfolded and folded states with no detectable intermediates. This type of two-state transition often has been studied by equilibrium methods (*17*−*19*). Typically, the protein is unfolded thermally or exposed to varied concentrations of a perturbant, such as urea or guanidinium, while a spectroscopic signal from the folded state is monitored.

Only a few experimental studies of membrane protein unfolding have been reported. Bacteriorhodopsin is quite resistant to thermal unfolding. Purple membrane undergoes a transition at approximately 100 °C at pH 6, measured by differential scanning calorimetry (*20*). Although the retinal chromophore is bleached above this transition, substantial secondary structure remains (*21*). The calorimetric transition shifts to 80 °C at pH 6 for bacteriorhodopsin solubilized in CHAPS[1]/DMPC micelles (*22*). An extensive series of experiments on bacterioopsin folding have been reported by Booth and co-workers (*23*). Folding was observed on a millisecond to second time scale when SDS-solubilized bacterioopsin was mixed with CHAPS/DMPC micelles along with the retinal chromophore, and several folding intermediates were identified. Similar studies were also reported by Chen and Gouaux (*24*), who showed that the bacterioopsin folding transition from SDS to CHAPSO/DMPC was reversible. The authors of these studies point out that SDS-solubilized bacterioopsin is only partially unfolded, containing substantial helix content. The helical segments in SDS may be similar to those in the native structure, as suggested by the NMR structure of an SDS-solubilized proteolytic fragment of bacteriorhodopsin (*25*). SDS-induced partial

† Supported by grants from the National Institutes of Health (GM 08194) and the San Antonio Area Foundation.

* To whom correspondence should be addressed at the Department of Biology, University of Texas at San Antonio. E-mail: RRenthal@UTSA.edu. Tel: 210-458-5452.

‡ University of Texas at San Antonio.

§ University of Texas Health Science Center at San Antonio.

[1] Abbreviations: CHAPS, 3-[(3-cholamidopropyl)dimethylammonio]-1-propanesulfonate; DMPC, dimyristoylphosphatidylcholine; CHAPSO, 3-[(3-cholamidopropyl)dimethylammonio]-2-hydroxy-1-propanesulfonate; SDS, sodium dodecyl sulfate; C1, bateriorhodopsin fragment containing residues 72−248; C2, bacteriorhodopsin fragment containing residues 1−71; FRET, Förster-type resonance energy transfer.

10.1021/bi034875c CCC: $27.50
Published on Web 12/17/2003

unfolding of diacylglycerol kinase was reported by Lau and Bowie (*26*). The data were fit to a linear free energy model. A potentially serious drawback of SDS as a membrane protein denaturant is the evident inapplicability of thermodynamic models which have been worked out in detail for water-soluble proteins. Tanford (*17*) related the free energy change for urea- or guanidinium-induced unfolding of water-soluble proteins to the change in exposure of protein surface to solvent between the folded and unfolded states. Measurement of the free energy change requires that ΔG varies linearly with the denaturant concentration (*18*, *19*). In mixed micelles of neutral and anionic detergents, this condition is unlikely to be met, due to deviations from ideal mixing (*27*).

Previous studies reported complete unfolding of bacterioopsin in trifluoroacetic acid (*28*). Bacteriorhodopsin exposed to less aggressive solvents [formic acid and ethanol (*28*), various alcohols (*29*), or chloroform and methanol (*25*)] shows considerable helical structure, but helix−helix interactions appear to be disrupted. In this paper, we have explored the possible use of ethanol as a perturbant for studying bacterioopsin unfolding under equilibrium conditions. Unfolding is monitored by resonance energy transfer from tryptophan side chains to a dansyl group attached to Lys 41 (*30*).

EXPERIMENTAL PROCEDURES

Materials. Bacteriorhodopsin was obtained from purple membrane isolated from *Halobacterium salinarum* S9 as described by Oesterhelt and Stoeckenius (*31*). Dansyl chloride, CHAPS, octyl glucoside, and chymotrypsin were obtained from Sigma (St. Louis, MO). Dimyristoylphosphatidylcholine was obtained from Avanti Polar Lipids (Alabaster, AL). Ethanol was HPLC grade from Burdick and Jackson (Muskegon, MI). Formic acid (90%) was obtained from Baker (Phillipsburg, NJ).

Fluorescent Labeling. Purple membrane was specifically modified at Lys 41 with dansyl chloride as previously described (*30*, *32*). Dansylbacterioopsin was purified by dissolving lyophilized dansyl-purple membrane in 90% formic acid, diluting to 30% with ethanol (*33*), and chromatographing on LH-60 in $CHCl_3$/methanol (1:1) containing 0.1 M ammonium acetate (*5*). For spectra of the apomembrane, retinal was cleaved with hydroxylamine (*33*), and the retinal oxime was removed by washing with bovine serum albumin (*34*).

Chymotrypsin Cleavage. Dansyl chloride-modified purple membrane was cleaved with chymotrypsin between residues 71 and 72, and the resulting fragments, C1 (72−248) and dansyl-Lys 41 C2 (1−71), were separated by LH-60 chromatography in $CHCl_3$/methanol/ammonium acetate (*3*, *28*). Column fractions were dialyzed against 0.05 M phosphate, pH 6.0, and 0.2% sodium dodecyl sulfate (*5*).

Chymotrypsin Fragment Association. Dansyl-Lys 41 C2 in 0.2% sodium dodecyl sulfate and 0.05 M phosphate, pH 6.0, was mixed with varying amounts of C1 in the same buffer. To 0.4 mL of the C1−dansyl-Lys 41 C2 solution was added 0.15 mL of 2% CHAPS, 2% DMPC, and 0.05 M phosphate, pH 6.0. Under these conditions, the retinal chromophore is regenerable if *all-trans*-retinal is added (*35*). The final C2 concentration was 0.68 μM, and the final C1 concentration varied from 0 to 1.4 μM. In control experiments, unlabeled C2 was added to dansyl-Lys 41 C2.

Unfolding Experiments. Prior to fluorescence spectroscopy, column fractions were stored in $CHCl_3$/methanol/ammonium acetate at −20 °C at a concentration of 5 μM. Concentrations were determined by UV spectroscopy using an extinction coefficient of 65700 M^{-1} cm^{-1} at 280 nm (*36*). Aliquots of dansylbacterioopsin (0.07−0.11 nmol) were dried in 1.5 mL plastic tubes using a centrifugal evaporator. The residues were dissolved in 3 μL of 90% formic acid and diluted with 10 μL of ethanol. Various amounts of ethanol and water were added, along with detergent and acetate buffer, to a total volume of 1.0 mL. The final acetate concentration was 0.15 M. The pH of the acetate buffer in water was 5.6, but the amount of formic acid used to solubilize bacterioopsin lowered the pH to 4.51. The pH in the ethanolic solutions was not determined. The final detergent concentrations were 0.5% CHAPS/0.5% DMPC, 1 mM lauryl maltoside, or 40 mM octyl glucoside.

Fluorescence Spectroscopy. Fluorescence spectra were measured on a Farrand (Valhalla, NY) MK-I instrument, with corrected excitation, or a Photon Technology International (Lawrenceville, NJ) Quantamaster QM-4, with corrected excitation and emission. The Farrand MK-I was interfaced with a PC using a Data Translation (Marlboro, MA) 3010 analog-to-digital converter. Data were collected using Testpoint software (Capital Equipment Corp., Billerica, MA). Emission correction curves were generated from spectra of 2-aminopyridine, 2-naphthol, and quinine sulfate (*37*). These corrections were used to measure Q, the average quantum yield of tryptophan in bacterioopsin (0.14), and J, the spectral overlap between tryptophan and dansyl (4.28×10^{-15} M^{-1} cm^3). The Förster critical distance $R_0 = 9790(\kappa^2 n^{-4} QJ)^{1/6} =$ 21 Å, where κ^2, the dipole orientation factor, is taken as $^2/_3$, and n, the index of refraction of the medium, is taken as 1.4 (*38*). We previously measured the emission anisotropy of dansyl-Lys 41-bacteriorhodopsin (*30*), which sets the value of κ^2 to between 0.078 and 3.2, giving a range of R_0 between 15 and 28 Å (*38*). However, the actual value of κ^2 is likely to be closer to the random orientation value due to the two transition dipoles of tryptophan.

Light Scattering. Rayleigh scattering was measured on a Farrand MK-I fluorometer, with the excitation monochromator set at 285 nm and the emission monochromator scanned from 250 to 350 nm. The intensity of the Rayleigh scattering peak at 285 nm, minus the scattering peak from water or buffer, was used as a measure of micelle concentration. Samples were prepared the same as in the unfolding experiments, except no protein was added and the samples were filtered through a Milex HV 0.45 μm filter (Millipore, Billerica, MA). A series of octyl glucoside samples prepared in water (0−40 mM) was used to measure the critical micelle concentration. Micelle radii were estimated by dynamic light scattering using a DynaPro MS instrument (Proterion Corp., Piscataway, NJ).

Stopped-Flow Kinetics. Dansyl-Lys 41-bacterioopsin was prepared in 90% ethanol, 0.15 M acetate, pH 5.6, and 40 mM octyl glucoside and loaded into a 2.5 mL syringe on an Applied Photophysics, Inc. (Surrey, U.K.), SX 18MV instrument. A second 2.5 mL syringe contained aqueous 0.15 M acetate buffer, pH 5.6, and 40 mM octyl glucoside. Equal volumes of the two syringes were mixed (instrument dead time, about 1 ms). The fluorescence was monitored with a >390 nm cutoff filter using 285 nm excitation.

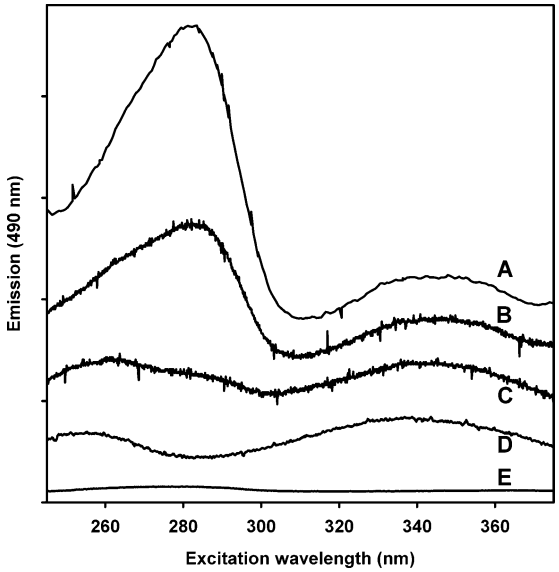

FIGURE 1: Förster-type resonance energy transfer (FRET) from bacterioopsin tryptophans to dansyl-Lys 41 as a folding signal. Dansyl emission was at 490 nm as a function of excitation wavelength. (A) Dansyl-Lys 41 bacterioopsin in purple membrane from which retinal chromophore was removed. (B) Dansyl-Lys 41 bacterioopsin in CHAPS/DMPC micelles. (C) Dansyl-Lys 41-bacterioopsin in 90% ethanol:10% water (containing CHAPS/DMPC). (D) Dansylmethylamine. (E) Same as (A) except the membrane was not labeled with the dansyl group.

RESULTS

Resonance Energy Transfer from Tryptophan to Dansyl-Lys 41 Measured by Sensitized Emission. Purple membrane was modified at Lys 41 with dansyl chloride and then bleached and treated with bovine serum albumin to remove retinal oxime, producing dansyl-Lys 41 white membrane. Excitation spectra, monitored at 490 nm, showed a strong peak of sensitized emission at 285 nm, suggesting tryptophan to dansyl Förster-type resonance energy transfer (Figure 1, upper line). Similar spectra were obtained for dansyl-Lys 41-bacterioopsin which had been unfolded in chloroform/methanol, separated from native lipids, and refolded in CHAPS/DMPC (Figure 1, middle line). Bacterioopsin prepared in this manner forms a nativelike chromophore when *all-trans*-retinal is added. The large sensitized emission peak at 285 nm suggests significant tryptophan to dansyl FRET.

The direct excitation peak of the dansyl group at 350 nm may be used as an internal standard to compare the two spectra. The stoichiometry of dansyl labeling of intact purple membrane was approximately 0.25 mol/mol. Thus, each trimer has only a single energy acceptor. Bacteriorhodopsin has eight Trp side chains (Figure 2). The expected resonance energy transfer efficiencies, *E*, between Trp and Lys 41 are shown in Table 1, calculated from $E = R_0^6/(R_0^6 + R^6)$ (*38*), where R = the distances between Lys 41 N_ζ and Trp C_ϵ in the high-resolution crystal structure [monomer (*39*); trimer (*40*)]. Assuming all Trp energy donors have the same quantum yield and assuming bacterioopsin in bleached purple membrane and CHAPS/DMPC micelles has the same tertiary structure as bacteriorhodopsin crystals, we estimated the energy transfer efficiency contributed by each Trp in a bacterioopsin monomer and in a singly dansyl-labeled trimer. The calculations (Table 1) show that the sum of transfer efficiencies for the bacteriorhodopsin trimer is 1.72; the sum of transfer efficiencies for the monomer is 0.957. Thus, the expected sensitized emission of bleached purple membrane should be 1.8 times that of a bacterioopsin monomer in CHAPS/DMPC. The results in Figure 1 are close to this value: for bleached dansyl-Lys 41-purple membrane, the ratio of 490 nm emission excited at 285 nm to that excited at 350 nm is 7.0. For dansyl-Lys 41-bacterioopsin in CHAPS/DMPC, the ratio is 3.5. Thus, the sensitized emission of the intact membrane (trimers of bacterioopsin) is 2.0 times that of monomers.

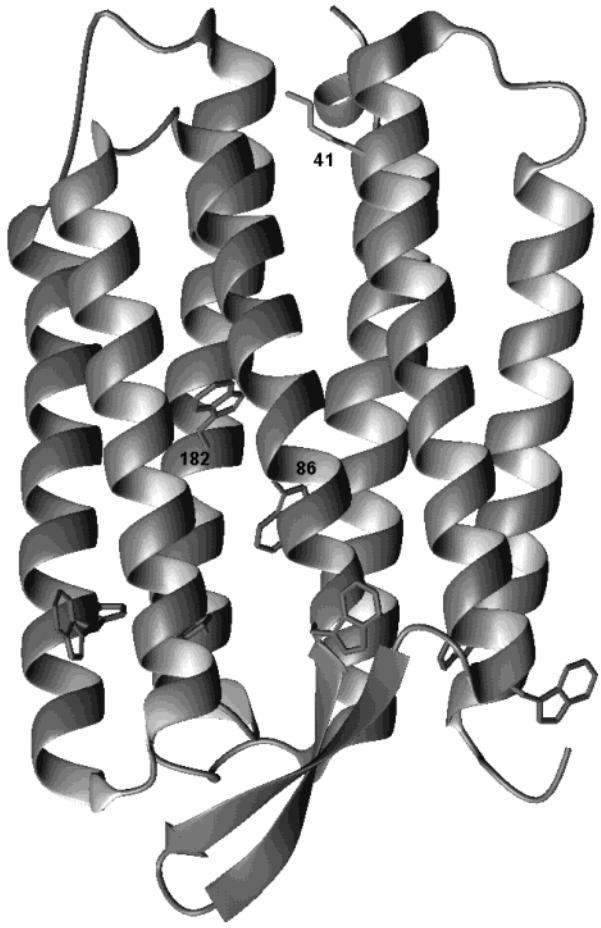

FIGURE 2: Structure of bacteriorhodopsin. Tryptophan fluorescence energy donors are shown, along with the location of the lysine side chain at position 41 to which the dansyl energy acceptor is attached. Only Trp 86 and 182 are close enough to the dansyl acceptor for substantial resonance energy transfer. This figure was prepared from PDB file 1C3W using MOLMOL (*55*).

Lipid-free dansyl-Lys 41-bacterioopsin dissolved in 90% ethanol (0.15 M acetate buffer, 0.5% CHAPS, 0.5% DMPC) shows virtually no sensitized emission at 285 nm (Figure 1, lower curve). There is only a small effect of ethanol on the Trp quantum yield of bacterioopsin, and the quantum yield of model dansyl compounds actually increases when the solvent is changed from water to ethanol (see below). Thus, the simplest explanation for the loss of the 285 nm sensitized emission is an increase in distance between the Trp donors and the dansyl acceptor. Trp 182, which is the closest Trp side chain to Lys 41, would have to move about 15 Å away from Lys 41 to produce the observed loss of transfer efficiency.

Tryptophan to Dansyl FRET Measures Helix−Helix Interactions. The quantum yields of the individual Trp side

Table 1: Distances (R) from Lys 41 to Bacteriorhodopsin Trp Residues (Lys N_ζ to Trp C_ϵ)[a]

	R, Å	E		R, Å	E
1brr			1c3w		
182A	20.5	0.53	182	20.3	0.55
86A	27.6	0.16	86	26.2	0.21
80A	33.0	0.06	80	33.0	0.06
138A	34.7	0.05	138	34.3	0.05
137A	35.7	0.04	137	35.7	0.04
12A	39.2	0.02	12	38.5	0.03
10A	42.1	0.02	10	41.9	0.02
182B	25.1	0.25	sum		0.96
86B	29.5	0.12			
137B	32.4	0.07			
138B	34.5	0.05			
189B	35.0	0.04			
80B	36.1	0.04			
12B	46.0	0.01			
10B	49.8	0.01			
182C	30.8	0.09			
86C	34.1	0.05			
80C	36.2	0.04			
137C	39.0	0.02			
189C	40.7	0.02			
138C	42.3	0.01			
12C	48.3	0.01			
10C	49.7	0.01			
sum		1.72			

[a] Fluorescence energy transfer efficiency (E) was calculated from $E = R_0^6/(R_0^6 + R^6)$ with $R_0 = 21$ Å. Data for the bacteriorhodopsin trimer were from PDB file 1BRR and the monomer from PDB file 1C3W.

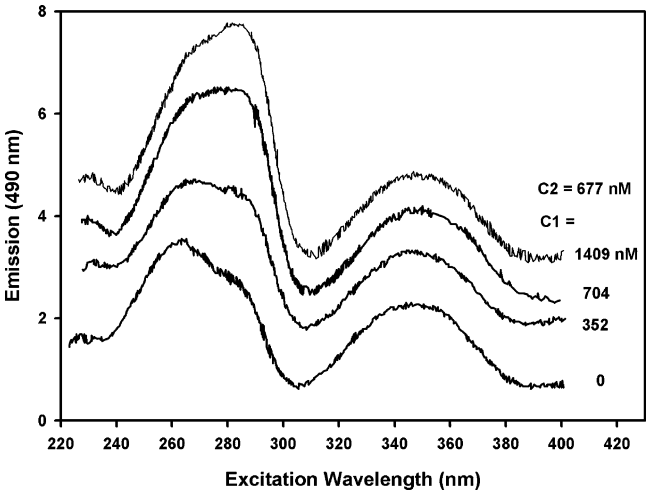

FIGURE 3: Fluorescence excitation spectra showing interaction between two proteolytic fragments of bacterioopsin, C1 (amino acids 72−248) and C2 (1−71). C2 is labeled with the dansyl group at position 41. Sensitized emission at 285 nm indicates that C1 and C2 are interacting.

chains are not known. However, it is possible to separately measure the energy transfer from Trp 10 and 12 to dansyl-Lys 41 after separating residues 1−71 from residues 72−248 by chymotrypsin cleavage and chromatography. The excitation spectrum of the resulting C2 fragment is shown in Figure 3 (lowest line).

Addition of increasing amounts of the chymotrypsin fragment C1, containing the nearest Trp donors in the folded bacteriorhodopsin structure, results in an increase in the sensitized emission, suggesting formation of a complex between C1 and C2. The C1·C2 complex is capable of forming a nativelike purple chromophore upon addition of *all-trans*-retinal (*3*, *28*). The equilibrium can be displayed

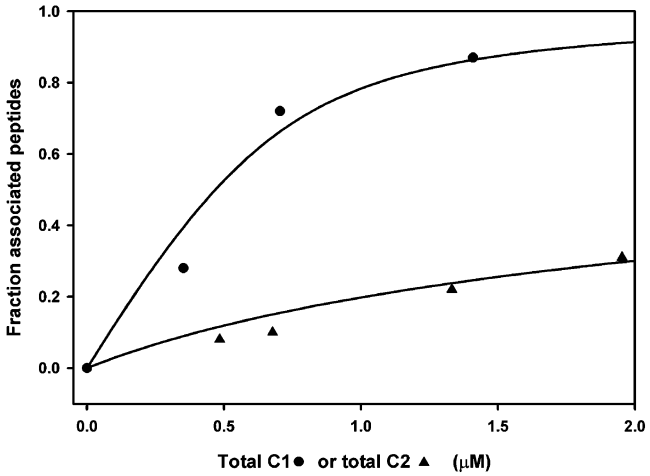

FIGURE 4: Apparent association of C1 and C2 fragments (circles and upper curve) and self-association of C2 (triangles and lower curve), measured by FRET. C1−C2 association data, from Figure 3, were analyzed as described in the text. The line was calculated from eq 5. C2 self-association data were analyzed by an equation analogous to eq 5.

quantitatively by assuming that the sensitized emission at 285 nm (as a ratio to the 350 nm emission) will reach a limiting value of 3.5 (see Figure 1). Also, we assume that the sensitized emission in the absence of C1 is 0. Actually, there is a small amount of sensitized emission (Figure 3, lower curve). This is due to some C2 dimer (data not shown). Neglecting the dimer, we assume that the ratio of 285 nm excited emission to 350 nm excited emission ranges from 0 to 3.5. The association constant may be estimated from these data as follows:

$$\mathrm{C1} + \mathrm{C2} \leftrightarrows \mathrm{C1{\cdot}C2} \quad (1)$$

$$K = [\mathrm{C1{\cdot}C2}]/([\mathrm{C1}][\mathrm{C2}]) \quad (2)$$

$$\text{sensitized emission} \propto \text{fraction C2 bound to C1} = f_{C2} = [\mathrm{C1{\cdot}C2}]/([\mathrm{C1{\cdot}C2}] + [\mathrm{C2}]) \quad (3)$$

$$\text{sensitized emission} \propto \text{fraction C2 bound to C1} = K(\mathrm{C1_T} - f_{C2}\mathrm{C2_T})/[K(\mathrm{C1_T} - f_{C2}\mathrm{C2_T}) + 1] \quad (4)$$

where $C1_T$ and $C2_T$ are the total concentrations of C1 and C2. Solving for f_{C2} gives

$$f_{C2} = (1 + K(\mathrm{C1_T} + \mathrm{C2_T}) - ((1 + K(\mathrm{C1_T} + \mathrm{C2_T}))^2 - 4K^2\mathrm{C1_T}\mathrm{C2_T})^{0.5})/2K\mathrm{C2_T} \quad (5)$$

The value of f_{C2} is obtained from the 285 nm sensitized emission peak on the assumption that $f_{C2} = 1.0$ corresponds to the spectrum obtained for intact bacterioopsin in CHAPS/DMPC (Figure 1, middle curve) and $f_{C2} = 0$ corresponds to the spectrum of C2 in the absence of C1 (Figure 3, lower curve). Thus, the only unknown in eq 5 is the association constant, K. The best fit for C1−C2 association, shown in Figure 4, was $K = 7.7 \times 10^6\ \mathrm{M}^{-1}$. A similar analysis of the self-association of C2 gives an association constant of $0.15 \times 10^6\ \mathrm{M}^{-1}$.

Equilibrium Unfolding in Ethanol. To observe the transition between the nearly folded bacterioopsin in CHAPS/DMPC (Figure 1, middle curve) and the ethanol-perturbed form of bacterioopsin in ethanol (Figure 1, lower curve), we

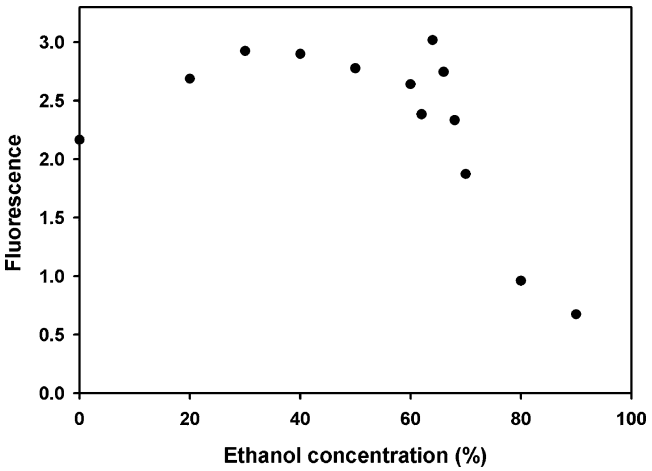

FIGURE 5: Variation of FRET (Trp donors, dansyl-Lys 41 acceptor) with ethanol concentration. Excitation wavelength: 285 nm. Emission wavelength: 500 nm. All samples contained 0.1% CHAPS, 0.1% DMPC, and 0.15 M acetate, pH 5.6. Normalized to constant dansyl emission (see Figure 8).

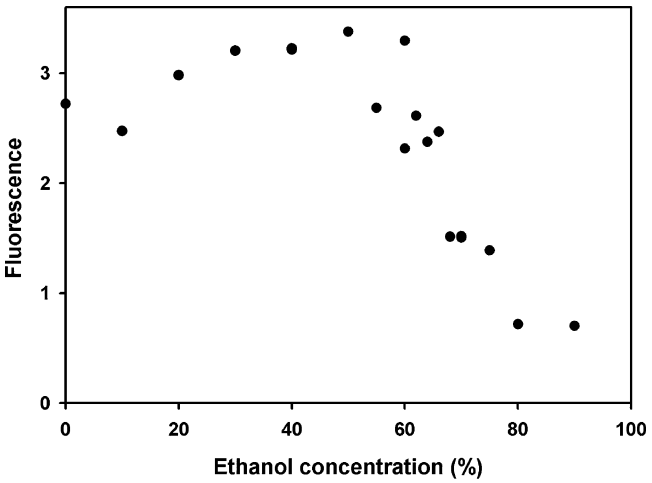

FIGURE 6: Variation of FRET (Trp donors, dansyl-Lys 41 acceptor) with ethanol concentration. Same conditions as in Figure 5, except samples are in 1% octyl glucoside. Normalized to constant dansyl emission (see Figure 8).

prepared samples of bacterioopsin containing 0.5% CHAPS, 0.5% DMPC, and varying amounts of ethanol. The fluorescence excitation spectra of these samples are shown in Figure 5. Up to about 60% ethanol, the magnitude of the FRET signal, measured by sensitized emission at 500 nm from 285 nm excitation, increases as the ethanol concentration increases. Above 60% ethanol, the FRET signal sharply decreases to nearly 0. This transition suggests that the fluorescence donor and acceptor are being separated by an unfolding process. Similar to CHAPS/DMPC, bacterioopsin also refolds into the native conformation in octyl glucoside micelles when retinal is added (*41*). Therefore, we also looked at the effect of added ethanol on the Trp to dansyl-Lys 41 FRET signal in octyl glucoside micelles. The results are shown in Figure 6. The ethanol concentration at which the FRET signal has decreased by 50% is nearly the same in both octyl glucoside and CHAPS/DMPC. Tyrosine-to-tryptophan energy transfer does not influence the results, as the same transition is observed when sensitized emission from 295 nm excitation is measured as a function of ethanol concentration (data not shown).

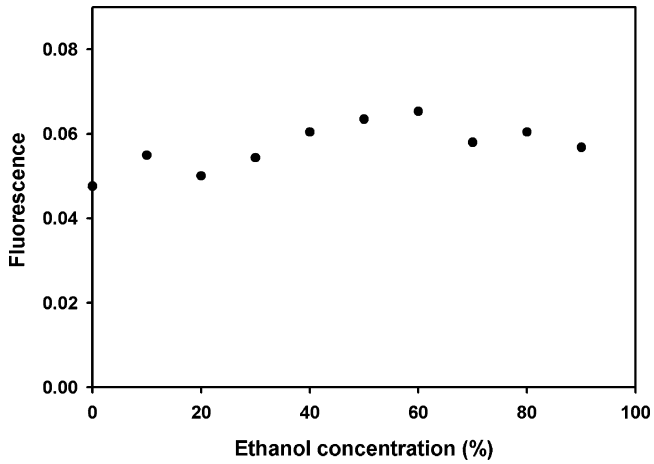

FIGURE 7: Effect of ethanol on bacterioopsin Trp fluorescence. Same conditions as in Figure 6 except with unmodified bacterioopsin (lacking dansyl modification at Lys 41). Fluorescence emission was measured at 332 nm from 285 nm excitation.

Solvent Effects on Tryptophan and Dansyl. Because both tryptophan and dansyl are known to undergo changes in fluorescence quantum yield in solvents of different polarities, it was necessary to study the effects of varying ethanol concentration on tryptophan and dansyl emission. As the ethanol concentration increases, a shift is observed (uncorrected) in the maximum emission wavelength of bacterioopsin tryptophans, from 326 nm in aqueous octyl glucoside to 335 nm in octyl glucoside/80% ethanol (data not shown). The variation of tryptophan emission at 332 nm in bacterioopsin in octyl glucoside as a function of ethanol concentration is shown in Figure 7. There is a small increase in quantum yield up to about 60% ethanol, beyond which there is a small decrease. The decrease above 60% ethanol is not sufficient to account for the large decrease in sensitized emission observed in Figures 5 and 6, unless (a) a single tryptophan is responsible for most of the sensitized emission and (b) that tryptophan, but not any other one, undergoes nearly complete solvent quenching above 60% ethanol. The selectivity of such a set of conditions seems unlikely, considering the major contributors to the FRET signal (Figure 1 and Table 1): Trp 182 and Trp 86 are closest to the dansyl-Lys 41 acceptor, but both are among the most buried tryptophans in bacteriorhodopsin. The more exposed tryptophans are more likely to experience large changes in quantum yield with change in solvent. The small changes observed could be interpreted to indicate that the environment of the tryptophans in the folded protein is not appreciably different from a solvent composed of 70−90% ethanol.

The fluorescence of the dansyl group is expected to vary with solvent composition. In 40 mM octyl glucoside, dansyl-*N*-methylamide undergoes a nearly 10-fold enhancement in quantum yield between 0% and 90% ethanol (data not shown). The dansyl group at Lys 41 in bacterioopsin, based on the observed change in quantum yield with ethanol concentration (Figure 8), is unlikely to be in a completely aqueous environment in the absence of added ethanol. It appears that the dansyl group in partially unfolded bacterioopsin (i.e., above 60% ethanol) may be in a more polar environment than in the folded protein. The magnitude of resonance energy transfer from tryptophan to dansyl depends on the quantum yield of tryptophan and the absorbance of

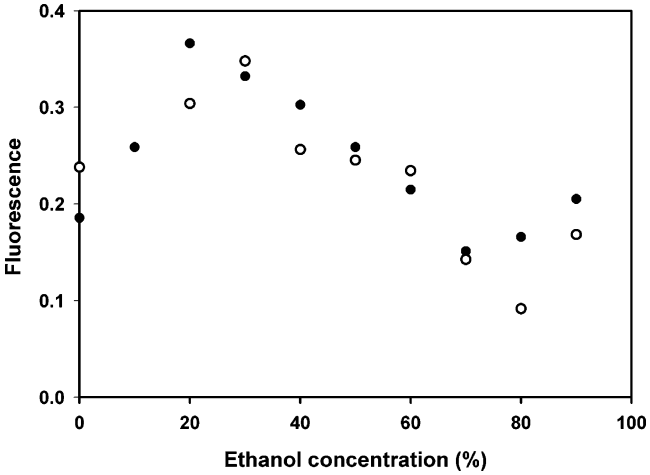

FIGURE 8: Effect of ethanol on dansyl fluorescence in dansyl-Lys 41-bacterioopsin. Similar conditions as in Figures 5 and 6 except for direct excitation of the dansyl group at 340 nm. Key: open circles, dansyl-Lys 41-bacterioopsin in CHAPS/DMPC; filled circles, dansyl-Lys 41-bacterioopsin in octyl glucoside. Fluorescence emission was measured at 500 nm.

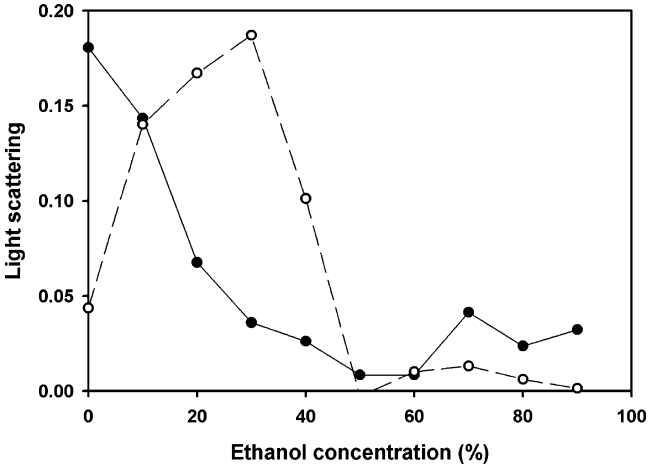

FIGURE 9: Changes in micelle concentration and/or size as a function of ethanol concentration. Detergent and buffer concentrations were the same as in Figures 5 and 6 except no bacterioopsin was added. Key: filled circles, octyl glucoside; open circles, CHAPS/DMPC.

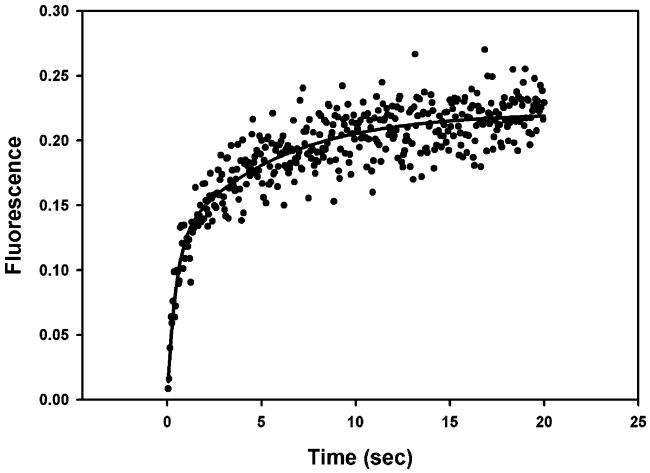

FIGURE 10: Stopped-flow kinetics of bacterioopsin folding monitored by FRET (tryptophan donors, dansyl-Lys 41 acceptor). Two 2.5 mL syringes contained either aqueous 0.15 M acetate buffer, pH 5.6, and 40 mM octyl glucoside or dansyl-Lys 41-bacterioopsin in 90% ethanol, 0.15 M acetate buffer, pH 5.6, and 40 mM octyl glucoside. Excitation: 285 nm. Emission: >390 nm. The line was fit to $A[1 - \exp(-k_1 t)] + B[1 - \exp(-k_2 t)]$, where $A = 0.119$, $k_1 = 2.32\ s^{-1}$, $B = 0.103$, and $k_2 = 0.185\ s^{-1}$. Correlation coefficient = 0.80.

the dansyl group. However, the measurement of FRET by sensitized emission to assay protein folding assumes the quantum yield of the energy acceptor does not vary with the state of unfolding. Thus, in Figures 5 and 6, the FRET signal has been normalized by dividing the spectra by the emission from 340 nm excitation to correct for the observed changes in dansyl emission as it varies with solvent conditions (Figure 8). The change in the dansyl environment at about 20−30% ethanol may represent a change in protein structure that affects the area around Lys 41 but does not affect the tryptophan to dansyl donor−acceptor distances.

Solvent Effects on Octyl Glucoside Micelles. The transition observed in resonance energy transfer above 60% ethanol (Figures 5 and 6) could be a secondary effect resulting from a change in detergent micelle structure, rather than a direct solvent−protein interaction. Therefore, we examined the micelle systems for effects of ethanol concentration. We measured light scattering as a probe of micelle concentration. The light scattering method was tested by using it to measure the critical micelle concentration of octyl glucoside, which was found to be 22 mM [close to the value of 21.8 mM obtained by Walter et al. (*42*)]. The results are shown in Figure 9. Added ethanol diminishes the light scattering from octyl glucoside, and the micelles appear to be disrupted above 20% ethanol. The dissipation of micelles was confirmed by dynamic light scattering, which showed a decrease in micelle radius from 2.6 nm in water to a broad distribution of sizes less than 2.0 nm at 10% and 20% ethanol. No micelles were detected at 30% or higher ethanol concentrations. By contrast, the CHAPS/DMPC system is more complicated. As ethanol is added, there is a sharp increase in scattering, suggesting the formation of large aggregates. These aggregates appear to be completely disrupted when the ethanol concentration reaches 50%. The changes in bacterioopsin conformation observed by FRET (Figures 5 and 6) occur above 60% ethanol. Therefore, it is unlikely that the ethanol concentration dependence of changes in resonance energy transfer efficiency is a process related to micelle dissociation. In both detergent systems, there do not appear to be any micelles remaining above 60% ethanol, where the dansyl probe signals a large transition.

Kinetic Folding. The kinetics of folding was examined by stopped-flow fluorometry. Aqueous octyl glucoside was mixed with an equal volume of octyl glucoside in 90% ethanol containing dansyl-Lys 41-bacterioopsin. The signal was selected to measure the appearance of FRET by exciting at 285 nm and collecting fluorescence above 390 nm. An increase in fluorescence was observed on a time scale of a few seconds (Figure 10). No change in the signal was observed when the aqueous and 90% ethanol buffered detergent solutions were mixed in the absence of dansyl-Lys-41-bacterioopsin. The kinetic process observed in Figure 10 corresponds to jumping across the FRET transition shown in Figure 6, from 90% ethanol to 45% ethanol. The fluorescence increase in Figure 10 was fitted to two exponentials: a fast fluorescence increase (rate constant = 2.32

s^{-1}) and a slower increase (0.185 s^{-1}). The weighting factors for the two processes are approximately equal (ratio of faster to slower process 0.54 to 0.46).

DISCUSSION

FRET from Tryptophans to Dansyl-Lys 41 in Bacterioopsin. Förster-type resonance energy transfer (FRET) can be used to detect proximity between parts of a protein (*38*). As a result of FRET, the fluorescence of an energy donor is quenched by a nearby energy acceptor via a dipole resonance interaction. If the acceptor is itself fluorescent, then emission will be observed from the acceptor when the donor is excited (sensitized emission). We previously found that, near neutral pH, dansyl chloride exclusively modifies Lys 41 of bacteriorhodopsin (*30*, *32*). The Förster critical distance for energy transfer from tryptophan to dansyl is 21 Å (distance at which 50% of the emission is transferred to the acceptor). Thus, the tryptophan−dansyl donor−acceptor pair is useful in the distance range of helix−helix interactions. We used tryptophan to dansyl FRET to detect formation of long-range interactions in bacterioopsin folding or loss of long-range interactions in bacterioopsin unfolding. Bacteriorhodopsin has eight tryptophans (Figure 2). However, only Trp 86 and Trp 182 are close enough to the dansyl acceptor in the folded protein to contribute appreciably to the energy transfer efficiency (Table 1).

Although the three-dimensional structure of bacteriorhodopsin is known at high resolution (*39*), the structure of bacterioopsin (the apoprotein lacking the retinal chromophore) is not known. Some studies suggest that the structures are similar. When the retinal chromophore was removed from purple membrane, the conformation of bacterioopsin was found by NMR to be similar to that of bacteriorhodopsin (*43*). Also, the temperature dependence of the rate of chromophore regeneration from *all-trans*-retinal plus apomembrane is consistent with only a small conformational change, similar to formation of bacteriorhodopsin from the M photocycle intermediate (*35*). The conformation of purified bacterioopsin in CHAPS/DMPC micelles or octyl glucoside micelles is also unknown. In both of these micelle systems, the purple chromophore may be regenerated by addition of *all-trans*-retinal (*28*, *41*, *44*). This suggests that bacterioopsin is folded into a conformation close to the native state. Bacteriorhodopsin exists as a monomer in CHAPS/DMPC (*22*) and in octyl glucoside (*45*). In CHAPS/DMPC, the helical content, as measured by circular dichroism, is close to that of the native state (*3*, *4*, *28*, *41*, *46*). There is some evidence that bacteriorhodopsin is unstable in octyl glucoside (*47*, *48*). Thus, the protein conformation is close to, although probably not identical to, that known for bacteriorhodopsin.

We observe FRET from tryptophan to dansyl-Lys 41 in bacterioopsin (Figure 1). The approximately 2-fold difference between FRET of associated bacterioopsin in bleached purple membrane and monomeric bacterioopsin in CHAPS/DMPC and in octyl glucoside detergent micelles is consistent with the assumption that the conformation of bacterioopsin in detergent is compact and similar to the native conformation. We observe relatively little sensitized emission when purified dansylbacterioopsin is dissolved in ethanol (Figure 1), suggesting that, in ethanol, the helices containing the tryptophan donors have moved far away from the helix containing the dansyl acceptor. Previous NMR studies of two-helix fragments of bacterioopsin in chloroform/methanol indicate that the helices are intact, but the helix−helix interactions have been lost (*25*).

The interaction between bacterioopsin helices has been previously observed in the absence of large-scale unfolding by examining the association between two proteolytic fragments, C1 and C2 (*3*, *4*, *41*). We found that a two-helix fragment, C2, shows little sensitized emission (Figure 3), but in the presence of the remaining five helices (C1), the sensitized emission increases, indicating formation of a C1·C2 complex. We used this signal to estimate the association constant between C1 and C2 as 7.7×10^6 M^{-1} (Figure 4). The standard free energy change is thus −9.3 kcal/mol.

Ethanol-Induced Unfolding. We measured the transition between the state of bacterioopsin in aqueous detergent micelles (strong tryptophan to dansyl FRET) and the state of bacterioopsin in ethanol (weak tryptophan to dansyl FRET) as a function of ethanol concentration. The transition was found to be rather sharp, occurring between 60% and 70% ethanol in both CHAPS/DMPC (Figure 5) and octyl glucoside (Figure 6). In both detergents, the micelles have become solubilized at ethanol concentrations well below the transition (Figure 9), suggesting that the transition represents a solvent effect directly on the protein stability. The observed changes are not due to solvent effects on the tryptophan quantum yield, since it changes little over the entire range of ethanol concentrations (Figure 7). The simplest interpretation of the ethanol-induced change in FRET is that bacterioopsin undergoes an unfolding transition above 60% ethanol, increasing the distance between the dansyl energy acceptor on Lys 41 and the nearest tryptophan side chains in the folded bacterioopsin structure, Trp 86 and Trp 182. This transition is not likely to involve complete unfolding of helices, since bacterioopsin and subfragments retain nearly full helicity in organic solvent (*28*, *25*).

Apparent Free Energy of Unfolding. Perturbant-induced unfolding of water-soluble proteins has been studied in great detail (*17*, *18*). For simple two-state transitions, one may calculate an equilibrium constant from the unfolding curve and extrapolate the free energy change to zero perturbant concentration, thus obtaining an apparent free energy change of unfolding. Assuming a two-state transition (F, folded, and U, unfolded), the equilibrium constant K for unfolding can be calculated as a function of denaturant concentration (E):

$$\mathrm{F} \leftrightarrows \mathrm{U} \tag{6}$$

$$K_E = [\mathrm{U}]/[\mathrm{F}] \tag{7}$$

At a particular denaturant concentration, the free energy change for unfolding is (*19*)

$$\Delta G_E = -RT \ln K_E \tag{8}$$

where R is the gas constant and T the absolute temperature. The value of the free energy change for unfolding at zero denaturant concentration, ΔG_{H_2O}, can be obtained by extrapolation, using (*19*, *49*)

$$\Delta G_E = \Delta G_{H_2O} + m[\mathrm{E}] \tag{9}$$

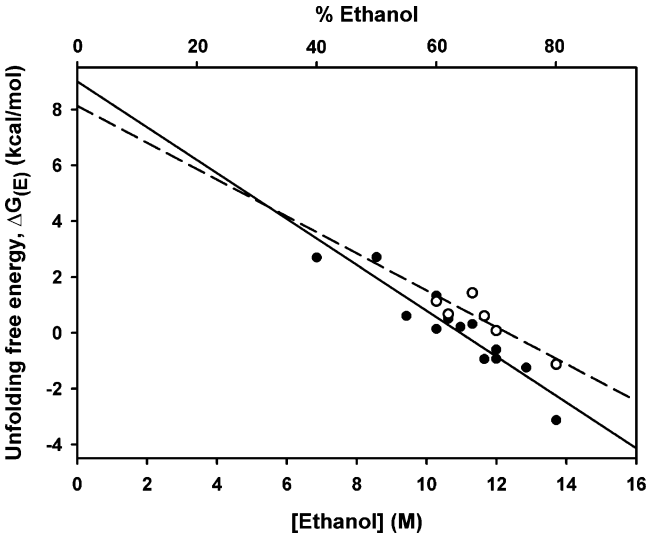

FIGURE 11: Extrapolation of free energy of unfolding to zero denaturant concentration (see eq 9). Key: filled circles and solid line, octyl glucoside data (from Figure 6); open circles and dashed line, CHAPS/DMPC data (from Figure 5). Least-squares lines have correlation coefficients of 0.88 (solid line) and 0.78 (dashed line).

where m is the free energy change for unfolding per mole per liter of denaturant. The data in Figure 6 (octyl glucoside) were replotted according to eq 9 in Figure 11, assuming a two-state equilibrium. The slope is $m = -0.8$ kcal mol^{-1} M^{-1}, and the intercept is $\Delta G_{H_2O} = 9.0$ kcal/mol. A similar plot (not shown) for Figure 5 (CHAPS/DMPC) gives a slope of $m = -0.7$ kcal mol^{-1} M^{-1} and an intercept of $\Delta G_{H_2O} = 8.1$ kcal/mol. These values are of the same order of magnitude as measurements of these parameters for water-soluble proteins (for example, refs *50* and *51*). However, the unfolding process measured for water-soluble proteins includes both tertiary and secondary structure unfolding.

Two models for the ethanol-induced unfolding of bacterioopsin are shown in Figure 12. The figure shows the helices as if they are intact in both the folded and unfolded states. However, as discussed above, the helix content may be less than that in the native state. In the upper model, all of the helices have separated. In the lower model, a small hinge motion has occurred at the connecting loop between helices B and C, which separates the dansyl fluorescence acceptor at Lys 41 from the two closest tryptophan fluorescence donors, Trp 182 and Trp 86. Future fluorescence labeling studies incorporating fluorescent probes at engineered cysteines in helix connecting loops could distinguish between these two possibilities.

Folding Kinetics. Using stopped-flow spectrofluorometry, we measured the rate of folding from 90% ethanol to 45% ethanol (Figure 10). The data are best fit by two kinetic components, one with a half-time of about 0.3 s and the other with a half-time of about 3.7 s, with approximately equal weighting factors. Further experiments will be required to characterize the two kinetic processes observed. There are several possible explanations that could be considered: (1) One explanation is two separate partial folding events, a fast rate sensed by one tryptophan and a slower rate sensed by another. For example, if the partially unfolded state corresponds to the product of pathway I in Figure 12, then when bacterioopsin folds, Trp 86 in helix C might quickly approach dansyl-Lys 42 in helix B, while Trp 182 in helix F more slowly approaches helix C. (2) Another explanation is that

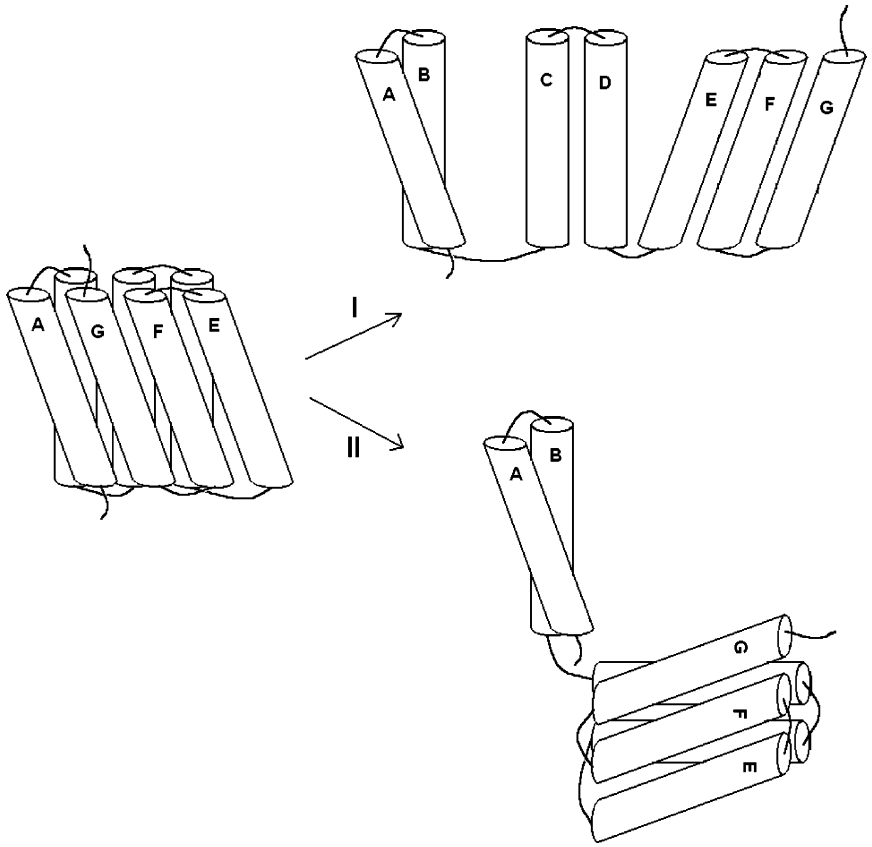

FIGURE 12: Two possible unfolding pathways for bacterioopsin in ethanol. Transmembrane helices are lettered with the N-terminal helix = A and the C-terminal helix = G.

a preexisting equilibrium may occur in the unfolded state, between different partially unfolded forms which have different folding kinetics, similar to the pH-dependent equilibrium observed by Lu and Booth (*52*). If the kinetic components represent formation and decay of an intermediate folding state of bacterioopsin which is present at equilibrium, or if multiple folded or unfolded states exist which fold by separate kinetic processes, then the two-state assumption used in the analysis of Figures 5 and 6 is invalid. Future kinetic studies covering the transition region of Figures 5 and 6 might clarify this. Helix association in the folding of water-soluble proteins is a much faster process than the rates measured for bacterioopsin in Figure 10. The observed rates of bacterioopsin folding are closer to the time scale observed for domain assembly in water-soluble proteins. Multidomain water-soluble proteins display complex folding mechanisms (*53*). Popot and de Vitry (*54*) have argued that a single transmembrane helix, containing around 25 amino acids, should be considered a domain, comparable to the 70 amino acid domains typically found in small water-soluble proteins.

Booth and co-workers studied the refolding kinetics of bacterioopsin that had been partially unfolded in dodecyl sulfate and detected two intermediate states, I_1 and I_2 (*23*). The formation of I_1 occurs on the same time scale as the faster of the two rates we observe in folding of bacterioopsin from ethanol (Figure 10). Intermediate I_2 forms with a rate constant in the range of 0.01 s^{-1}, which is an order of magnitude slower than the slow process we observed in folding from ethanol (Figure 10). Formation of I_2 was found to coincide with increase in helical content (*46*). Since alcohols are known helix stabilization agents, it is not expected that an increase in helix content would be observed on refolding, and this may be a fundamental difference between unfolding in dodecyl sulfate and ethanol.

Conclusion. The process monitored by disappearance of tryptophan to dansyl FRET is likely to be ethanol-induced helix−helix dissociation. Further evidence for this conclusion comes from a comparison of the free energy of unfolding measured by ethanol denaturation (8−9 kcal/mol) and the free energy of association of the proteolytic fragments C1 and C2 (9 kcal/mol). The free energy changes are consistent with the two processes being similar.

ACKNOWLEDGMENT

We thank Barry Nall and Paul Horowitz for helpful discussions, Bettie Sue Masters for providing generous access to the Applied Photophysics stopped-flow instrument, Satya Panda and Linda Roman for assistance with the stopped-flow measurements, and Eileen Lafer for help with the dynamic light scattering measurements.

REFERENCES

1. Popot, J.-L., and Engelman, D. M. (2000) Helical membrane protein folding, stability, and evolution, *Annu. Rev. Biochem. 69*, 881−922.
2. Rees, D. C., DeAntonio, L., and Eisenberg, D. (1989) Hydrophobic organization of membrane proteins, *Science 245*, 510−513.
3. Liao, M. J., London, E., and Khorana, H. G. (1983) Regeneration of the native bacteriorhodopsin structure from two chymotryptic fragments, *J. Biol. Chem. 258*, 9949−9955.
4. Liao, M.-J., Huang, K.-S., and Khorana, H. G. (1984) Regeneration of native bacteriorhodopsin structure from fragments, *J. Biol. Chem. 259*, 4200−4204.
5. Sigrist, H., Wenger, R. H., Kislig, E., and Wuthrich, M. (1988) Refolding of bacteriorhodopsin. Protease V8 fragmentation and chromophore reconstitution from proteolytic V8 fragments, *Eur. J. Biochem. 177*, 125−133.
6. Gilles-Gonzalez, M. A., Engelman, D. M., and Khorana, H. G. (1991) Structure−function studies of bacteriorhodopsin XV. Effects of deletions in loops B−C and E−F on bacteriorhodopsin chromophore and structure, *J. Biol. Chem. 266*, 8545−8550.
7. Kahn, T. W., and Engelman, D. M. (1992) Bacteriorhodopsin can be refolded from two independently stable transmembrane helices and the complementary five-helix fragment, *Biochemistry 31*, 6144−6151.
8. Marti, T. (1998) Refolding of bacteriorhodopsin from expressed polypeptide fragments, *J. Biol. Chem. 273*, 9312−9322.
9. Kim, J.-M., Booth, P. J., Allen, S. J., and Khorana, H. G. (2001) Structure and function in bacteriorhodopsin: the role of the interhelical loops in the folding and stability of bacteriorhodopsin, *J. Mol. Biol. 308*, 409−422.
10. Zhou, F. X., Cocco, M. J., Russ, W. P., Brunger, A. T., and Engelman, D. M. (2000) Interhelical hydrogen bonding drives strong interactions in membrane proteins, *Nat. Struct. Biol. 7*, 154−160.
11. Zhou, F. X., Merianos, H. J., Brunger, A. T., and Engelman, D. M. (2001) Polar residues drive association of polyleucine transmembrane helices, *Proc. Natl. Acad. Sci. U.S.A. 98*, 2250−2255.
12. Dawson, J. P., Weinger, J. S., and Engelman, D. M. (2002) Motifs of serine and threonine can drive association of transmembrane helices, *J. Mol. Biol. 316*, 799−805.
13. Lemmon, M. A., and Engelman, D. M. (1992) Specificity and promiscuity in membrane helix interactions, *FEBS Lett. 346*, 17−20.
14. Mall, S., Broadbridge, R., Sharma, R. P., East, J. M., and Lee, A. G. (2001) Self-association of model transmembrane α-helices is modulated by lipid structure, *Biochemistry 40*, 12379−12386.
15. Yano, Y., Takemoto, T., Kobayashi, S., Yasui, H., Sakurai, H., Ohashi, W., Niwa, M., Futaki, S., Sugiura, Y., and Matsuzaki, K. (2002) Topological stability and self-association of a completely hydrophobic model transmembrane helix in lipid bilayers, *Biochemistry 41*, 3073−3080.
16. Renthal, R., and Velasquez, D. (2002) Self-association of helical peptides in a lipid environment, *J. Protein Chem. 21*, 255−264.
17. Tanford, C. (1970) Protein denaturation. C. Theoretical models for the mechanism of denaturation, *Adv. Protein Chem. 24*, 1−95.
18. Schellman, J. A. (1978) Solvent denaturation, *Biopolymers 17*, 1305−1322.
19. Pace, C. N. (1986) Determination and analysis of urea and guanidine hydrochloride denaturation curves, *Methods Enzymol. 131*, 266−280.
20. Brouillette, C. G., Muccio, D. D., and Finney, T. K. (1987) pH dependence of bacteriorhodopsin thermal unfolding, *Biochemistry 26*, 7431−7438.
21. Taneva, S. G., Caaveiro, J. M. M., Muga, A., and Goni, F. M. (1995) A pathway for the thermal destabilization of bacteriorhodopsin, *FEBS Lett. 367*, 297−300.
22. Brouillette, C. G., McMichens, R. B., Stern, L. J., and Khorana, H. G. (1989) Structure and thermal stability of monomeric bacteriorhodopsin in mixed phospholipid/detergent micelles, *Proteins 5*, 38−46.
23. Booth, P. J. (2000) Unraveling the folding of bacteriorhodopsin, *Biochim. Biophys. Acta 1460*, 4−14.
24. Chen, G. Q., and Gouaux, E. (1999) Probing the folding and unfolding of wild-type and mutant forms of bacteriorhodopsin in micellar solutions: evaluation of reversible unfolding conditions, *Biochemistry 38*, 15380−15387.
25. Pervushin, K. V., Orekhov, V. Yu., Popov, A. I., Musina, L. Yu., and Arseniev, A. S. (1994) Three-dimensional structure of (1−71) bacterio-opsin solubilized in methanol/chloroform and SDS micelles determined by $^{15}N-^{1}H$ heteronuclear NMR spectroscopy, *Eur. J. Biochem. 219*, 571−583.
26. Lau, F. W, and Bowie, J. U. (1997) A method for assessing the stability of a membrane protein, *Biochemistry 36*, 5884−5892.
27. Tanford, C. (1980) *The hydrophobic effect*, 2nd ed., p 93, J. Wiley and Sons, NY.
28. Huang, K. S., Bayley, H., Liao, M. J., London, E., and Khorana, H. G. (1981) Refolding of an integral membrane protein. Denaturation, renaturation, and reconstitution of intact bacteriorhodopsin and two proteolytic fragments, *J. Biol. Chem. 256*, 3802−3809.

29. Mitaku, S., Ikuta, K., Itoh, H., Katoaka, R., Naka, M., Yamada, M., and Suwa, M. (1988) Denaturation of bacteriorhodopsin by organic solvents, *Biophys. Chem. 30*, 69−79.
30. Renthal, R., Cothran, M., Dawson, N., and Harris, G. (1987) Fluorescent labeling of purple membrane: implications for helix connections, *Biochim. Biophys. Acta 897*, 384−394.
31. Oesterhelt, D., and Stoeckenius, W. (1974) Isolation of the cell membrane of *Halobacterium halobium* and its fractionation into red and purple membrane, *Methods Enzymol. 31*, 667−678.
32. Harris, G., Renthal, R., Tuley, J., and Robinson, N. (1979) Dansylation of bacteriorhodopsin near the retinal attachment site, *Biochem. Biophys. Res. Commun. 91*, 926−931.
33. Gerber, G. E., Anderegg, R. J., Herlihy, W. C., Gray, C. P., Biemann, K., and Khorana, H. G. (1979) Partial primary structure of bacteriorhodopsin: sequencing methods for membrane proteins, *Proc. Natl. Acad. Sci. U.S.A. 76*, 227−231.
34. Katre, N. V., Wolber, P. K., Stoeckenius, W., and Stroud, R. M. (1981) Attachment site(s) of retinal in bacteriorhodopsin, *Proc. Natl. Acad. Sci. U.S.A. 78*, 4068−4072.
35. Renthal, R., and Alaniz, C. (1999) Conformational change in bacterio-opsin on binding to retinal, *Biophys. Chem. 78*, 241−245.
36. Renthal, R., and Haas, P. (1996) Effect of transmembrane helix packing on tryptophan and tyrosine environments in detergent-solubilized bacterio-opsin, *J. Protein Chem. 15*, 281−289.
37. Melhuish, W. H. (1973) Absolute spectrofluorometry, in *Accuracy in Spectrophotometry and Luminescence Measurements*, *Natl. Bur. Stand., Spec. Publ. 378*, 137−150.
38. Stryer, L. (1978) Fluorescence energy transfer as a spectroscopic ruler, *Annu. Rev. Biochem. 47*, 819−846.
39. Luecke, H., Schobert, B., Richter, H. T., Cartailler, J. P., Lanyi, J. K. (1999) Structure of bacteriorhodopsin at 1.55 A resolution, *J. Mol. Biol. 291*, 899−911.
40. Essen, L.-O., Siegert, R., Lehmann, W. D., and Oesterhelt, D. (1998) Lipid patches in membrane protein oligomers: crystal structure of the bacteriorhodopsin-lipid complex, *Proc. Natl. Acad. Sci. U.S.A. 95*, 11673−11678.
41. London, E., and Khorana, H. G. (1982) Denaturation and renaturation of bacteriorhodopsin in detergents and lipid-detergent mixtures, *J. Biol. Chem. 257*, 7003−7011.
42. Walter, A., Kuehl, G., Barnes, K., and VanderWaerdt, G. (2000) The vesicle-to-micelle transition of phosphatidylcholine vesicles induced by nonionic detergents: effects of sodium chloride, sucrose and urea, *Biochim. Biophys. Acta 1508*, 20−33.
43. Yamaguchi, S., Tuzi, S., Tanio, M., Naito, A., Lanyi, J. K., Needleman, R., and Saito, H. (2000) Irreversible conformational change of bacterio-opsin induced by binding of retinal during its reconstitution to bacteriorhodopsin, as studied by ^{13}C NMR, *J. Biochem. 127*, 861−869.
44. Braiman, M. S., Stern, L. J., Chao, B. H., and Khorana, H. G. (1987) Structure−function studies on bacteriorhodopsin. IV. Purification and renaturation of bacterio-opsin polypeptide expressed in *Escherichia coli*, *J. Biol. Chem. 262*, 9271−9276.
45. Lustig, A., Engel, A., Tsiotis, G., Landau, E. M., and Baschong, W. (2000) Molecular weight determination of membrane proteins by sedimentation equilibrium at the sucrose or nycodenz-adjusted density of the hydrated detergent micelle, *Biochim. Biophys. Acta 1464*, 199−206.
46. Riley, L. M., Wallace, B. A., Flitsch, S. L., and Booth, P. J. (1997) Slow α helix formation during folding of a membrane protein, *Biochemistry 36*, 192−196.
47. Mao, D., and Wallace, B. A. (1984) Differential light scattering and absorption flattening optical effects are minimal in the circular dichroism spectra of small unilamellar vesicles, *Biochemistry 23*, 2667−2673.
48. Muccio, D. D., and DeLucas, L. J. (1985) Isolation of detergent-solubilized monomers of bacteriorhodopsin by size-exclusion high-performance liquid chromatography, *J. Chromatogr. A 326*, 243−250.
49. Santoro, M. M., and Bolen, D. W. (1988) Unfolding free energy changes determined by the linear extrapolation method. 1. Unfolding of phenylmethanesulfonyl α-chymotrypsin using different denaturants, *Biochemistry 27*, 8063−8068.
50. Baskakov, I. V., and Bolen, D. W. (1998) Monitoring the sizes of denatured ensembles of staphylococcal nuclease proteins: implications regarding *m* values, intermediates, and thermodynamics, *Biochemistry 37*, 18010−18017.
51. Ramos, C. H. I., Kay, M. S., and Baldwin, R. L. (1999) Putative interhelix ion pairs involved in the stability of myoglobin, *Biochemistry 38*, 9783−9790.
52. Lu, H., and Booth, P. J. (2000) The final stages of folding of the membrane protein bacteriorhodopsin occur by kinetically indistinguishable parallel folding paths that are mediated by pH, *J. Mol. Biol.* (2000) 233−243.
53. Privalov, P. L. (1989) Thermodynamic problems of protein structure, *Annu. Rev. Biophys. Biophys. Chem. 18*, 47−69.
54. Popot, J.-L., and de Vitry, C. (1990) On the microassembly of integral membrane proteins, *Annu. Rev. Biophys. Biophys. Chem. 19*, 369−403.
55. Koradi, R., Billeter, M., and Wüthrich, K. (1996) MOLMOL: a program for display and analysis of macromolecular structures, *J. Mol. Graphics 14*, 51−55.

BI034875C